Engineering Notes

ENGINEERING NOTES are short manuscripts describing new developments or important results of a preliminary nature. These Notes cannot exceed 6 manuscript pages and 3 figures; a page of text may be substituted for a figure and vice versa. After informal review by the editors, they may be published within a few months of the date of receipt. Style requirements are the same as for regular contributions (see inside back cover).

Orbital Dynamics of the Hanging Tether Interferometer

Anthony B. DeCou*
Northern Arizona University,
Flagstaff, Arizona 86001

Introduction

ASTRONOMICAL observations using long baseline optical interferometry in space are theoretically possible using numerous methods that have been examined at various levels of detail in recent years.[1,2] One possible method that has not received significant attention is the use of a three mass gravity-gradient-stabilized tethered system in circular orbit. This system consists of two radiation collecting telescopes located at the ends of the tether and a central station (CS) which measures the coherence of the sampled beams and is located on a movable platform that moves along the tether to equalize the optical path lengths of the two beams at all times. Whether or not this will prove to be practical depends in part on whether the motions of the components of the system can be stabilized in the presence of various disturbing forces with the accuracy necessary to perform interferometry. The most important of these disturbances are the Coriolis forces associated with the movement of the central station and vibrations introduced into the system by both the tether reeling mechanism and the platform crawling mechanism. This Note examines the consequences of Coriolis forces and leaves the analysis of vibrations caused by mechanical components for a later time. A strategy for canceling the Coriolis forces using ion thrusters is analyzed and shown to use thrust levels and fuel levels that are easily within the present state of the art for a 10-km baseline interferometer operating in synchronous orbit.

U-V Plane Coverage

The geometry of the system in an operating mode is shown in Fig. 1 in which $\bar{i},\bar{j},\bar{k}$ is a triad of Earth-centered "inertial" unit vectors. The vector $\bar{l}$ extends from the lower collector to the upper collector and nominally rotates at the orbital rate ω_0 around the $\bar{k}$ direction that is perpendicular to the orbit plane. The direction of observation on the celestial sphere defines another inertial system in which $\bar{k}_1$ is a unit vector in the direction of observation and the unit vectors $\bar{i}_1,\bar{j}_1$ define the "*U-V*" plane in which the Fourier transform of the image is sampled by measuring the visibility and phase of fringes. Without loss of generality, $\bar{i}$ and $\bar{i}_1$ may be fixed in the same direction. The angle ϕ between $\bar{k}$ and $\bar{k}_1$ varies between 0 and 180 deg enabling the system to view the entire celestial sphere.

The position on the *U-V* plane sampled at any instant of time $\bar{D}(t)$ (called the baseline vector of the sample) is the projection of the vector $\bar{l}$ on the *U-V* plane, and is given by

$$\bar{D}(t) = l\left[\sin(\omega_0 t)\bar{i}_1 + \cos\phi\,\cos(\omega_0 t)\bar{j}_1\right] \tag{1}$$

Received Jan. 26, 1990; revision received April 29, 1990; accepted for publication May 7, 1990.

*Associate Professor of Engineering; also Summer Faculty Fellow 1988–1989 at the Jet Propulsion Laboratory.

where l is the length of the tether. This is the locus of an ellipse for which the eccentricity is equal to $1/\cos\phi$. Thus, coverage of the *U-V* plane is most uniform when the source direction is perpendicular to the orbit plane, and deteriorates to a straight line in the direction parallel to the orbit plane. Coverage of a complete ellipse requires one orbital period. A complete observation of one source would require many orbits using different tether lengths, resulting in a series of concentric ellipses of arbitrary size. This is identical to the shape and the rate of coverage of the *U-V* plane achievable using the free-flyer approach to interferometry.[3]

The final sample distribution in the *U-V* plane is determined by the fringe sampling rate along the ellipses and the spacing between ellipses. The former is determined by the built-in system parameters (including the orbital rate) and the intensity of the source, none of which are under the immediate control of the user. The spacing between the ellipses on the other hand can be actively controlled by the user to influence the sampling distribution by varying the tether length. How this control might be utilized to achieve specific sampling objectives is the subject of another paper.[4]

Coriolis Force Disturbances

It is clear from Fig. 1 that unless $\phi = 0$ the central station (CS) must continuously move up and down the tether at the orbital rate in order to keep the optical path lengths of the two legs of the interferometer equal. The vertical motion of the CS will pull (or push) the two collectors in the opposite direction with respect to the center of mass (CM) of the entire system. If we assume that the CM is in a circular orbit, which is a reasonable approximation, then all three masses will experience Coriolis forces in the rotating coordinate system according to the well-known equation

$$\bar{F} = -2M\omega_0 V\bar{l}_\perp \tag{2}$$

where $\bar{l}_\perp$ is the unit vector in the orbit plane perpendicular to the tether in the direction of orbital motion, and V is the vertical velocity, positive in the upward direction. When the CS is moving upward, it will tend to fall behind in the orbit while the two collectors that are being pulled down are tending to get ahead. A computer simulation using the tether dynamics program GTOSS with animated output has been used to verify the general appearance of the resulting motion. It clearly shows that if these forces are unopposed, they will cause large

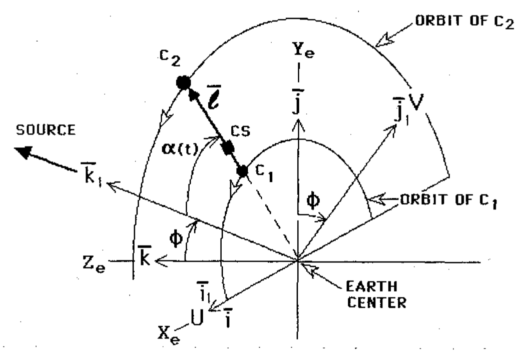

Fig. 1 Linear three-mass gravity gradient stabilized system in which the $\bar{i},\bar{j}$ unit vectors define the orbit plane in inertial space and $\bar{i}_1,\bar{j}_1$ define the *U-V* plane for a source in direction $\bar{k}_1$ on the celestial sphere.

distortions and vibrations in the tether which are incompatible with the interferometer requirements. Theoretically, one could compensate for this by making the motion of the CS more complicated, but the vibrations induced in the tether and the increased complexity required in the optical system would undoubtedly defeat this approach.

Therefore, it is assumed that the application of thrust to the CS and/or the collectors will be required to oppose the Coriolis forces. It is also assumed that this thrusting will be continuous and of the type that could be provided by ion thrusters, rather than impulsive, because the forces being opposed are continuous. Impulsive thrusting applied frequently enough might maintain the approximate linear shape of the system, but it would also introduce unwanted vibrations and almost certainly use more fuel than the ion-thruster system. The purpose of the rest of this section is to determine an ion-thrusting strategy that will oppose and cancel the Coriolis forces. The maximum thrust, and the total ΔV required to implement the strategy, will also be derived.

To determine the force on each mass using Eq. (2), it is first necessary to find V as a function of time and relevant system parameters. Referring to Fig. 2, the angle α between $\bar{l}$ and the unit vector $\bar{k}_1$ in the source direction is given by

$$\cos\alpha = (1/l)(\bar{k}_1 \cdot \bar{l}) = \sin\phi \cos(\omega_0 t) \tag{3}$$

The relative position of the CS along the tether $x(t)$ is determined by the requirement that the optical path length $y(t)$ from the upper collector to the CM be equal to the path length $x(t) + \cos(\alpha)$ from the lower collector as shown in Fig. 2. Therefore, since $l = x(t) + y(t)$, we may use Eq. (3) to get

$$x(t) = (l/2)\left[1 - \sin\phi \cos(\omega_0 t)\right] \tag{4}$$

so when $\phi = 0$, the CS is stationary in the middle of the tether, and when $\phi = 90$ deg, the motion is sinusoidal between the two ends. The distance of the center of mass $X_{\rm CM}(t)$ from the lower collector is easily shown to be

$$X_{\rm CM}(t) = K_C l + K_{\rm CS} x(t) \tag{5}$$

where $K_C = M_C/(2M_C + M_{\rm CS}) = M_C/M_t$ and $K_{\rm CS} = M_{\rm CS}/M_t$ are the ratios of the collector mass and the CS mass to the total system mass. Since this local coordinate system is attached to the lower collector, the vertical velocities of the collectors and the CS with respect to the center of mass, are given, respectively, by

$$V_C = -\dot{X}_{\rm CM}(t) = -K_{\rm CS}\dot{x}(t) \tag{6}$$

$$V_{\rm CS} = \dot{x}(t) - \dot{X}_{\rm CM}(t) = 2K_C \dot{x}(t) \tag{7}$$

The force vector on each of the collectors and on the central station is found by combining Eqs. (2), (6), (7) and the derivative of Eq. (4) resulting in

$$F_C = l\omega_0^2 K_C K_{\rm CS} M_t \sin\phi \sin(\omega_0 t)\bar{l}_\perp \tag{8}$$

$$\bar{F}_{\rm CS} = -2\bar{F}_C \tag{9}$$

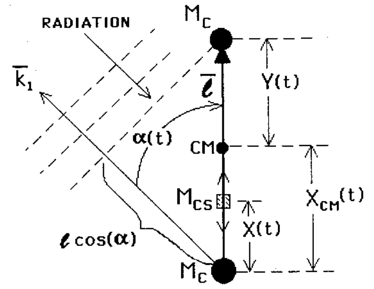

Fig. 2 Required motion of the CS and the CM relative to the lower collector.

The force on the CS is always twice the force on the collectors in the opposite direction. The total system impulse (I_t) required to oppose these forces and keep the tether straight and vertical for one orbital period T, corresponding to a full cycle in the U-V plane, is given by

$$I_t = 2\int_0^T |\bar{F}|\,dt + \int_0^T |\bar{F}_{\rm CS}|\,dt = 16 l\omega_0 K_C K_{\rm CS} M_t \sin\phi \tag{10}$$

A measure of system merit is the overall ΔV_t defined by

$$\Delta V_t = I_t/M_t = 16 l\omega_0 K_C K_{\rm CS} \sin\phi \tag{11}$$

It should be kept in mind that we have ignored the Coriolis forces on the tether, which has been assumed to be massless. A practical way to remove this assumption and also reduce total impulse is to let the Coriolis forces on the collectors and the tether go unopposed and apply sufficient thrust on the CS to equate its acceleration to the acceleration of the rest of the system at all times. The entire system will then speed up and slow down every ¼ orbit making the path of CM slightly noncircular. This will in turn induce small librations in the gravity gradient system, but these librations will be of minor importance. A more detailed analysis of this alternative will not be attempted here except to derive the appropriate formula for ΔV_t. This is done by noting from Eq. (8) that the acceleration of the tether and collectors moving together with no opposing thrusting is given by $\bar{a}_C = \bar{F}_C/M_C$. In order to match this acceleration, the thrust applied to the CS must be

$$\bar{F}_{\rm CS}' = -\bar{F}_{\rm CS} + M_{\rm CS}\bar{a}_c = l\omega_0^2 M_{\rm CS} \sin\phi \sin(\omega_0 t)\bar{l}_\perp \tag{12}$$

This results in a total $\Delta V_t'$ per orbit of

$$\Delta V_t' = I_t'/M_t = 4 l\omega_0 K_{\rm CS} \sin\phi \tag{13}$$

which is less than the value required by the other approach by the factor $4K_C$. This approach might be a significant improvement, but it requires carrying all of the fuel on the CS, which will decrease K_C and could conceivably reduce $4K_C$ to a value less than one if fuel is the primary mass component.

From Eq. (12), the maximum required thrust is $F_{\rm max} = l\omega_0^2 M_{\rm CS} \sin\phi$. Typical parameters for an interferometer operating in synchronous orbit where $\omega_0 = 7.27 \times 10^{-5}$ rad/s, using a $l = 10$ km baseline, and a $M_{\rm CS}$ of 1000 kg, looking at a source in the orbit plane gives $F_{\rm max} = 0.053$ N. This thrust is easily available with existing ion thrusters. However, if this same system were to operate in low Earth orbit, $F_{\rm max} = 12.0$ N which is outside our present capabilities using a single-ion engine.

The fuel requirements for each orbit can be found by noting that the impulse is given by $I_t = M_f V_f$ in which M_f is the fuel mass required for a single orbit and V_f is the exhaust velocity. Combining this with Eq. (12) gives

$$M_f/M_{\rm CS} = 4l\omega_0 \sin\phi/V_f \tag{14}$$

Using the same parameters as previously and an exhaust velocity of $V_f = 3.4 \times 10^4$ m/s, which is typical for xenon fuel-ion engines, gives $M_f/M_{\rm CS} = 8.56 \times 10^{-5}$ for the synchronous orbit case, and $M_f/M_{\rm CS} = 1.28 \times 10^{-3}$ for the low Earth orbit case. Over an extended period of time, the values of l and $\sin\phi$ would change greatly, so the average value of $M_f/M_{\rm CS}$ would be much less than the maximum values above. To get a rough estimate of expected mission lifetime, let us assume that $(l \sin\phi)_{\rm av} = 0.5\ (l \sin\phi)_{\rm max}$ and that 10% of the initial CS mass is fuel. This results in a lifetime of approximately 2.3×10^3 orbits or 6.5 yr in synchronous orbit, and 156 orbits or 10.4 days in low Earth orbit.

Tether Tension

Another dynamics problem that needs to be resolved is the question of adequate tether tension. The scenario analyzed above leaves open the possibility that the tether could go slack or operate with too little tension. This will occur if the vertical acceleration of the collectors discussed above is greater than the acceleration caused by the gravity gradient forces. The question can be resolved by comparing the required vertical acceleration of the collectors [found by differentiating Eq. (6)] to the vertical acceleration that is caused by gravity gradient forces. The first is easily found to be $a_c = \dot{V}_c = -K_{CS}(l/2)\omega_0^2 \sin\phi \cos(\omega_0 t)$. The gravity gradient acceleration at the ends of a two-mass dumbell with length l is given by $a_{gg} = 3l\omega_0^2$, so that the ratio (a_{gg}/a_C) is

$$(a_{gg}/a_C) = 6/[K_{CS} \sin\phi \cos(\omega_0 t)] \tag{15}$$

Since $K_{CS} < 1$, it is clear that the gravity gradient force will always be at least six times the minimum acceptable value and will usually be much greater than that.

Conclusions

The analysis above shows that the thrust magnitude and the fuel requirements necessary for a hanging tether interferometer with a 10-km baseline are well within the present "state of the art" for a system operating in synchronous orbit, but are questionable in low Earth orbit. The thrusting necessary to oppose Coriolis forces would probably be provided by ion thrusters operating continuously using the variable thrust program also derived above. The major unanswered questions affecting the practicality of the system concern vibrations induced in the tether by the CS crawling mechanism, the reeling mechanism, and perhaps by the ion thrusters. The magnitude of these vibrations and their effect on the optical system and the attitude-control system needs to be examined both analytically and experimentally. The analytical investigation is progressing and hopefully the experimental investigation will soon follow.

Acknowledgment

The analysis presented here was accomplished at JPL during the summer of 1989 as part of the Summer Faculty Fellowship Program. Many thanks to the staff at JPL, especially Paul Penzo, for numerous helpful suggestions.

References

[1]Stachnik, R., Melroy, P., and Arnold, D., "Multiple Spacecraft Michelson Stellar Interferometry," *SPIE Proceedings, Instrumentation in Astronomy V*, Vol. 445, 1984, p. 358.

[2]Anon., "Workshop on Optical Interferometry in Space," European Space Agency, Granada, Spain, SP-273, June 1987.

[3]DeCou, A. B., "Orbital Station Keeping for Multiple Spacecraft Interferometry," *Journal of Astronautical Sciences*, Vol. 39, No. 3, 1991, pp. 283–297.

[4]DeCou, A. B., "Long Baseline Optical Interferometry in Earth Orbit (System Comparisons)," *Proceedings of the SPIE 1990 Symposium on Astronomical Telescopes and Instrumentation for the 21st Century*, Feb. 11–17, 1990, pp. 626–638.

Krylov Model Reduction Algorithm for Undamped Structural Dynamics Systems

Tzu-Jeng Su* and Roy R. Craig Jr.†
University of Texas at Austin, Austin, Texas 78712

Introduction

KRYLOV vectors have been shown to form an efficient basis for eigenvalue analysis and model reduction of structural dynamics systems.[1-3] In Ref. 4, a Krylov model reduction algorithm is developed for a damped structural dynamics system described by a matrix second-order differential equation together with an output measurement equation. Numerical results have shown that Krylov-based reduced models have some advantages over normal mode reduced models in the application to structural control problems. The purpose of this Note is to present a Krylov model reduction algorithm for undamped systems. The undamped case covered in this Note supplements the damped case in Ref. 4, completing the work on Krylov model reduction methods.

The Krylov model reduction algorithm presented here has a feature similar to the Lanczos algorithm in Ref. 2. However, it is a more general case because the algorithm includes the output measurement equation. It is also shown that the Krylov model reduction method has an association with the well-known parameter-matching method for general linear systems.[5,6] The reduced-order model obtained by the Krylov model reduction algorithm proposed here is shown to match a set of parameters called low-frequency moments. For a general linear time-invariant system described by

$$\dot{z} = Az + Bu \qquad z \in R^n,\ u \in R^l \tag{1a}$$

$$y = Cz \qquad y \in R^m \tag{1b}$$

the low-frequency moments are defined by $CA^{-i}B$, $i = 1, 2, \ldots$, which are the coefficient matrices in the Taylor series expansion of the system transfer function. One advantage of using Krylov reduced models for structural control design is that the Krylov formulation can eliminate the control and observation spillover terms while leaving only the dynamic spillover terms to be considered.[4]

In this Note, first a theorem is used to show how the Krylov vectors can form a basis to produce a reduced model with moment-matching property. Then, based on the theorem, an efficient algorithm to generate Krylov vectors is developed.

Undamped Structural Dynamics Systems

An undamped structural dynamics system can be described by the input-output equations

$$M\ddot{x} + Kx = Pu \tag{2a}$$

$$y = Vx + W\dot{x} \tag{2b}$$

where $x \in R^n$ is the displacement vector; $u \in R^l$ is the input force vector; $y \in R^m$ is the output measurement vector; M and K are the system mass and stiffness matrices, respectively; P is the force distribution matrix; and V and W are the displacement and velocity sensor distribution matrices, respectively. In most practical cases, it may be assumed that l and m are much smaller than n.

Applying the Fourier transform to Eq. (2a) yields the frequency response solution $X(\omega) = (K - \omega^2 M)^{-1} PU(\omega)$, with $X(\omega)$ and $U(\omega)$ the Fourier transforms of x and u. If the system is assumed to have no rigid-body motion, then a Taylor series expansion of the frequency response around $\omega = 0$ is possible. Thus,

$$X(\omega) = (I - \omega^2 K^{-1}M)^{-1} K^{-1} PU(\omega) = \sum_{i=0}^{\infty} \omega^{2i} (K^{-1}M)^i K^{-1} PU(\omega) \tag{3}$$

Combining Eq. (2b) and Eq. (3), the system output frequency response can be expressed as

$$Y(\omega) = \sum_{i=0}^{\infty} [V(K^{-1}M)^i K^{-1}P + j\omega W(K^{-1}M)^i K^{-1}P] \omega^{2i} U(\omega) \tag{4}$$

In these expressions, $V(K^{-1}M)^i K^{-1}P$ and $W(K^{-1}M)^i K^{-1}P$ play roles similar to that of low-frequency moments in the first-order state-space formulation. Therefore, we have the following definition.

Definition 1. The low-frequency moments of an undamped structural dynamics system described by Eqs. (2) are

---

Received Oct. 26, 1989; revision received Jan. 18, 1990.

*Postdoctoral Fellow, Aerospace Engineering. Member AIAA.

†Professor, Aerospace Engineering and Engineering Mechanics. Fellow AIAA.